AN ENERGY PRESERVING/DECAYING SCHEME FOR CONSTRAINED NONLINEAR MULTIBODY SYSTEMS

Elisabet Lens and Alberto Cardona

Centro Internacional de Métodos Computacionales en Ingeniería
CIMEC-INTEC, Conicet-Universidad Nacional del Litoral,
Güemes 3450, 3000 Santa Fe, Argentina
email: acardona@intec.unl.edu.ar

Key Words: Time Integration, DAE Systems, Energy Preservation, Energy Dissipation.

Abstract. *In this work we describe several numerical time integration methods for multibody system dynamics: an energy preserving scheme and three energy decaying ones, which introduce high frequency numerical dissipation in order to annihilate the non desired high frequency oscillations. An exhaustive analysis of these four schemes is done, including their formulation, energy preserving and decaying properties, taking into account the presence of nonlinear algebraic constraints and the incrementation of finite rotations.*

1   INTRODUCTION

Integration of second order index 3 Differential-Algebraic Equations (DAE) may lead to numerical instability when an integration method of the Newmark family integration is used, because of the algebraic constraints. These constraints are the cause of unbounded linearly growing oscillations in the acceleration response (weak instability). If a high frequency dissipation is introduced this instability can be controlled in the linear regime e.g. HHT,[1] Hulbert α-generalized methods.[2]

In the non linear regime, the stability cannot be guaranteed by usual methods of analysis which are based on the properties of the system transition matrix. An alternative to ensure the stability of the solution is by means of schemes that verify the preservation of the total energy of the system at each time step. But this unconditional stability does not guarantee a satisfactory performance of the scheme because the spurious high frequency oscillations that may appear, e.g. with a sudden variation of stiffness or at a shock, are conserved all along the response, masking the answer.

It becomes necessary to develop alternative schemes. A methodology that leads in a systematic way to obtain energy dissipative integration schemes is Time Discontinuous Galerkin (TDG),[3] initially developed for hyperbolic equations. In an early work[4] we revisited an energy preserving scheme proposed by Géradin.[5] Now we take that scheme to build a new one that guarantees stability all along the numerical integration process and furthermore introduces numerical dissipation for the high frequency oscillation. The paper is organized as follows: in section 2 we formulate the problem. In section 4 an energy preserving integration algorithm is derived by using the Time Continuous Galerkin approximation. In section 5 three energy decaying integration algorithms are derived by using the Time Discontinuous Galerkin approximation. Every proposed algorithm is analyzed individually, using examples that are described in detail in section 3.

2   FORMULATION OF THE PROBLEM

Let us describe a conservative mechanical system in terms of N generalized coordinates $\boldsymbol{q}$ submitted to R algebraic constraints

$$\boldsymbol{\Phi}(\boldsymbol{q}) = \boldsymbol{0}. \tag{1}$$

Its dynamic properties can be derived from an appropriate description of the potential energy of the system $\mathcal{V} = \mathcal{V}(\boldsymbol{q})$ and of its kinetic energy, which can be put in quadratic form without loss of generality

$$\mathcal{K} = \frac{1}{2}\boldsymbol{v}^T \boldsymbol{M} \boldsymbol{v}. \tag{2}$$

The $(M \times M)$ inertia matrix $\boldsymbol{M}$ can be assumed constant, symmetric and positive definite since velocities $\boldsymbol{v}$ are expressed in a *material frame*. The latter are treated as quasi-coordinates and take thus the form of linear combinations of generalized coordinate time derivatives

$$\boldsymbol{v} = \boldsymbol{L}(\boldsymbol{q})\dot{\boldsymbol{q}}, \tag{3}$$

being $\boldsymbol{L}(\boldsymbol{q})$ a $(M \times N)$ matrix with $M \leq N$. This inequality covers the case in which the description of angular velocities is made in terms of redundant rotation parameters such as Euler parameters. In this case the redundancy between parameters has to be removed by adding appropriate constraints to the global set (1).

The motion equations result from the application of Hamilton's principle:

$$\delta \int_{t_1}^{t_2} \left\{ \frac{1}{2} \boldsymbol{v}^T \boldsymbol{M} \boldsymbol{v} - \boldsymbol{\mu}^T \left(\boldsymbol{v} - \boldsymbol{L}(\boldsymbol{q})\dot{\boldsymbol{q}}\right) - \mathcal{V}(\boldsymbol{q}) - \boldsymbol{\lambda}^T \boldsymbol{\Phi}(\boldsymbol{q}) \right\} dt = 0 \qquad (4)$$

We perform successively variations on the variables $\boldsymbol{\mu}$, $\boldsymbol{\lambda}$, $\boldsymbol{v}$ y $\boldsymbol{q}$.

- the variation of the multipliers $\boldsymbol{\mu}$ restores the velocity equations (3)

- variation of the multipliers $\boldsymbol{\lambda}$ restores the constraints set (1)

- the variation of the velocities $\boldsymbol{v}$ shows that the multipliers $\boldsymbol{\mu}$ have the meaning of generalized momenta

$$\boldsymbol{\mu} = \boldsymbol{M} \boldsymbol{v} \qquad (5)$$

- the variation of the generalized displacements $\boldsymbol{q}$ yields

$$\int_{t_1}^{t_2} \left\{ \delta \boldsymbol{q}^T \left(-\frac{\partial \mathcal{V}}{\partial \boldsymbol{q}} - \frac{\partial \boldsymbol{\Phi}^T}{\partial \boldsymbol{q}} \boldsymbol{\lambda} + \frac{\partial}{\partial \boldsymbol{q}} \left[(\boldsymbol{L}\dot{\boldsymbol{q}})^T \boldsymbol{\mu} \right] \right) + \delta \dot{\boldsymbol{q}}^T \boldsymbol{L}^T \boldsymbol{\mu} \right\} dt = 0 \qquad (6)$$

from which the dynamic equilibrium equations will be extracted.

Integration by parts of (6) yields

$$\left[\delta \boldsymbol{q}^T \boldsymbol{L}^T \boldsymbol{\mu} \right]_{t_1}^{t_2} + \int_{t_1}^{t_2} \delta \boldsymbol{q}^T \left\{ -\frac{\partial \mathcal{V}}{\partial \boldsymbol{q}} - \frac{\partial \boldsymbol{\Phi}^T}{\partial \boldsymbol{q}} \boldsymbol{\lambda} + \frac{\partial}{\partial \boldsymbol{q}} \left[(\boldsymbol{L}\dot{\boldsymbol{q}})^T \boldsymbol{\mu} \right] - \frac{d}{dt} \left(\boldsymbol{L}^T \boldsymbol{\mu} \right) \right\} dt = 0 \qquad (7)$$

The combination of (5) and (3) gives

$$\boldsymbol{\mu} = \boldsymbol{M} \boldsymbol{L}(\boldsymbol{q}) \dot{\boldsymbol{q}} \qquad (8)$$

then, the equations of motion become a first order DAE system, with variables $\boldsymbol{q}$, $\boldsymbol{\mu}$ and $\boldsymbol{\lambda}$:

$$\boldsymbol{L}^T \dot{\boldsymbol{\mu}} + \frac{\partial \mathcal{V}}{\partial \boldsymbol{q}} + \boldsymbol{B}^T \boldsymbol{\lambda} + \dot{\boldsymbol{L}}^T \boldsymbol{\mu} - \frac{\partial}{\partial \boldsymbol{q}} \left[(\boldsymbol{L}\dot{\boldsymbol{q}})^T \boldsymbol{\mu} \right] = \boldsymbol{0}$$

$$\boldsymbol{\mu} - \boldsymbol{M} \boldsymbol{L}(\boldsymbol{q}) \dot{\boldsymbol{q}} = \boldsymbol{0} \qquad (9)$$

$$\boldsymbol{\Phi}(\boldsymbol{q}) = \boldsymbol{0}$$

where $\boldsymbol{B} = \partial \boldsymbol{\Phi} / \partial \boldsymbol{q}$ is the Jacobian matrix of constraints. Note that the last two terms in (9-a) can be written as

$$\dot{\boldsymbol{L}}^T \boldsymbol{\mu} - \frac{\partial}{\partial \boldsymbol{q}} \left[(\boldsymbol{L}\dot{\boldsymbol{q}})^T \boldsymbol{\mu} \right] = \boldsymbol{G}(\boldsymbol{\mu}) \dot{\boldsymbol{q}} \qquad (10)$$

where the matrix $\boldsymbol{G}(\boldsymbol{\mu})$ has the following components:

$$G_{jp} = \sum_i \mu_i \left(\frac{\partial L_{ij}}{\partial q_p} - \frac{\partial L_{ip}}{\partial q_j} \right) \tag{11}$$

Skew-symmetry of $\boldsymbol{G}$ follows immediately. The final form of the equations of motion is thus:

$$\boldsymbol{L}^T \dot{\boldsymbol{\mu}} + \frac{\partial \mathcal{V}}{\partial \boldsymbol{q}} + \boldsymbol{B}^T \boldsymbol{\lambda} + \boldsymbol{G}(\boldsymbol{\mu})\dot{\boldsymbol{q}} = \boldsymbol{0}$$
$$\boldsymbol{\mu} - \boldsymbol{M}\boldsymbol{L}(\boldsymbol{q})\dot{\boldsymbol{q}} = \boldsymbol{0} \tag{12}$$
$$\boldsymbol{\Phi}(\boldsymbol{q}) = \boldsymbol{0}$$

3   TEST EXAMPLES

Four test examples were chosen in order to show the performance of the different algorithms in the nonlinear regime, also taking into account the presence of nonlinear constraints and the stiff character of the differential equation. These examples are:

a) **Nonlinear, unconstrained, non stiff problem:** a simple pendulum with one degree of freedom $q = \theta$. The expressions of kinetic and potential energies are written as:

$$\mathcal{K} = \frac{1}{2}m\dot{\theta}^2\ell^2 \qquad \mathcal{V} = (1 - \cos\theta)mgl$$

We adopt $m = 1$, $\ell = 1$ with $q_0 = \pi/2$ and $v_0 = 0$ as initial conditions.

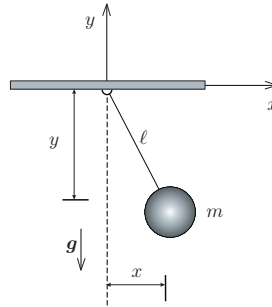Figure 1: The simple pendulum

b) **Nonlinear, constrained, non stiff problem:** a simple pendulum with two degrees of freedom $\boldsymbol{q}^T = [x \ y]$ and one nonlinear constraint $\Phi = x^2 + y^2 - \ell^2 = 0$. The expressions of the corresponding kinetic and potential energies are:

$$\mathcal{K} = \frac{1}{2}m(\dot{x}^2 + \dot{y}^2) \qquad \mathcal{V} = -mgy$$

We adopt $m = 1$ and $\ell = 1$. Initial conditions are $\boldsymbol{x}_0^T = [1 \ 0]$ and $\boldsymbol{v}_0^T = [0 \ 0]$.

c) **Nonlinear, constrained non stiff problem:** a double pendulum modelled with four degrees of freedom and nonlinear constraints:

$$\boldsymbol{q}^T = [x_1\ y_1\ x_2\ y_2\,] \qquad \boldsymbol{\Phi} = \begin{bmatrix} x_1^2 + y_1^2 - \ell_1^2 \\ (x_2 - x_1)^2 + (y_2 - y_1)^2 - \ell_2 \end{bmatrix}$$

The corresponding kinetic and potential energies expressions are

$$\mathcal{K} = \frac{1}{2}m_1(\dot{x}_1{}^2 + \dot{y}_1{}^2) + \frac{1}{2}m_2(\dot{x}_2{}^2 + \dot{y}_2{}^2) \qquad \mathcal{V} = m_1 g y_1 + m_2 g y_2$$

We adopt $m_1 = m_2 = 1$ and $\ell_1 = \ell_2 = 1$ with $\boldsymbol{x}_0^T = [1\ 0\ 1\ 1]$ and $\boldsymbol{v}_0^T = [0\ 0\ 0\ 0]$ as initial conditions.

d) **Nonlinear, constrained, stiff problem:** the same double pendulum of the previous item with a mass m_1 200 times smaller than m_2, forcing in this way an ill-conditioned mass matrix. We adopt $m_1 = 0.005$ and $m_2 = 1$.
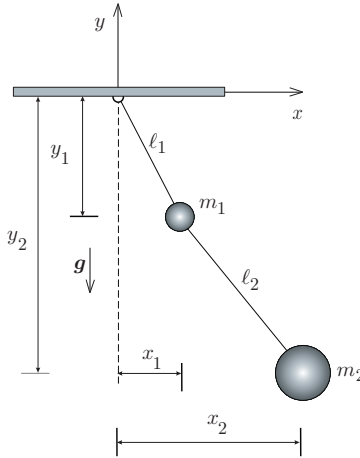

Figure 2: The double pendulum

4 THE TIME CONTINUOUS GALERKIN APPROXIMATION

4.1 Energy preserving scheme

4.1.1 Discretization of the equation of motion

In the Galerkin approximation the equations of motion are enforced in a weak (integral) manner. The Galerkin approximation of the equations of motion (12) is written as

$$\frac{h}{2} \int_{-1}^{1} \mathcal{W}_1(\tau) \left(\dot{\boldsymbol{q}} - \boldsymbol{L}^{-1}\boldsymbol{v} \right) d\tau +$$

$$\frac{h}{2} \int_{-1}^{1} \mathcal{W}_2(\tau) \left(\boldsymbol{M}\dot{\boldsymbol{v}} + \boldsymbol{L}^{-T}\boldsymbol{G}\dot{\boldsymbol{q}} + \boldsymbol{L}^{-T}\frac{\partial\mathcal{V}}{\partial\boldsymbol{q}} + \boldsymbol{L}^{-T}\boldsymbol{B}^T\boldsymbol{\lambda} \right) d\tau = \boldsymbol{0} \quad (13)$$
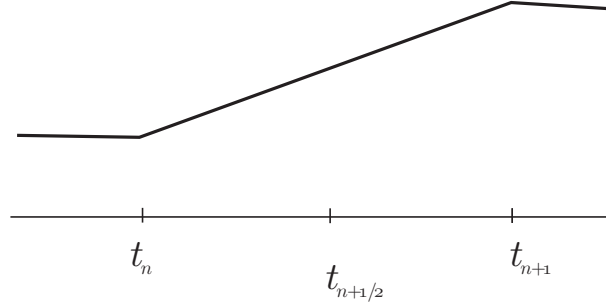
Figure 3: The time continuous Galerkin approximation of displacements and velocities

where $\mathcal{W}_i(\tau)$ are the weight functions, h is the time step size and τ a nondimensional time variable ($\tau = -1$ at t_n and $\tau = 1$ at t_{n+1}). By using piecewise linear interpolation functions for the displacements and velocities (Figure 3) and piecewise constant test functions $\mathcal{W}_1$ and $\mathcal{W}_2$, we obtain the set of discrete equations:

$$
\begin{cases}
\dfrac{1}{h}\boldsymbol{L}_{n+\frac{1}{2}}^T \boldsymbol{M}(\boldsymbol{v}_{n+1} - \boldsymbol{v}_n) + \dfrac{1}{h}\boldsymbol{G}_{n+\frac{1}{2}}(\boldsymbol{q}_{n+1} - \boldsymbol{q}_n) + \left.\dfrac{\partial \mathcal{V}}{\partial \boldsymbol{q}}\right|_{n+\frac{1}{2}} + \boldsymbol{B}_{n+\frac{1}{2}}^T \boldsymbol{\lambda}_{n+\frac{1}{2}} = \boldsymbol{0} \\[2mm]
\dfrac{1}{h}\boldsymbol{L}_{n+\frac{1}{2}}(\boldsymbol{q}_{n+1} - \boldsymbol{q}_n) = \dfrac{1}{2}(\boldsymbol{v}_{n+1} + \boldsymbol{v}_n) \\[2mm]
\boldsymbol{\Phi}_{n+1}(\boldsymbol{q}) = \boldsymbol{0}
\end{cases}
\tag{14}
$$

The matrix $\boldsymbol{L}_{n+\frac{1}{2}}$ will depend on the adopted rotation parametrization. The parametrization used (Euler parameters) assures a constant matrix $\boldsymbol{L}_{n+\frac{1}{2}}$ as it is shown in a previous work.[4]

4.1.2 Energy preservation in the discrete scheme

The total energy of the system is $\mathcal{E}(\boldsymbol{q}, \dot{\boldsymbol{q}}) = \mathcal{K}(\dot{\boldsymbol{q}}) + \mathcal{V}(\boldsymbol{q})$ where the kinetic energy has as a final expression $\mathcal{K} = \frac{1}{2}\boldsymbol{v}^T \boldsymbol{M} \boldsymbol{v}$ and the potential energy $\mathcal{V}(\boldsymbol{q})$ is function of the generalized coordinates $\boldsymbol{q}$. The total energy change in a time step can be evaluated computing the work done by the elastic, constraint and inertia forces.

To prove the total energy preservation of the discrete scheme, we multiply (14-a) by the displacements jump $(\boldsymbol{q}_{n+1} - \boldsymbol{q}_n)^T$ over a time step

$$
\frac{1}{h}(\boldsymbol{q}_{n+1} - \boldsymbol{q}_n)^T \boldsymbol{L}_{n+\frac{1}{2}} \boldsymbol{M}(\boldsymbol{v}_{n+1} - \boldsymbol{v}_n) + \frac{1}{h}(\boldsymbol{q}_{n+1} - \boldsymbol{q}_n)^T \boldsymbol{G}_{n+\frac{1}{2}}(\boldsymbol{q}_{n+1} - \boldsymbol{q}_n) +
$$

$$
(\boldsymbol{q}_{n+1} - \boldsymbol{q}_n)^T \left.\frac{\partial \mathcal{V}}{\partial \boldsymbol{q}}\right|_{n+\frac{1}{2}} + (\boldsymbol{q}_{n+1} - \boldsymbol{q}_n)^T \boldsymbol{B}_{n+\frac{1}{2}}^T \boldsymbol{\lambda}_{n+\frac{1}{2}} = 0 \quad (15)
$$

By looking at the first term we can identify the kinetic energy jump over a time step as:

$$
\frac{1}{h}(\boldsymbol{q}_{n+1} - \boldsymbol{q}_n)^T \boldsymbol{L}_{n+\frac{1}{2}} \boldsymbol{M}(\boldsymbol{v}_{n+1} - \boldsymbol{v}_n) = \frac{1}{2}(\boldsymbol{v}_{n+1} + \boldsymbol{v}_n)^T \boldsymbol{M}(\boldsymbol{v}_{n+1} - \boldsymbol{v}_n) = \mathcal{K}_{n+1} - \mathcal{K}_n \quad (16)
$$

Due to the skew-symmetry of the matrix $\boldsymbol{G}$ the second term becomes identically null.

$$\frac{1}{h}(\boldsymbol{q}_{n+1} - \boldsymbol{q}_n)^T \boldsymbol{G}_{n+\frac{1}{2}}(\boldsymbol{q}_{n+1} - \boldsymbol{q}_n) = \boldsymbol{0} \tag{17}$$

In the term of elastic forces derived from the potential $\mathcal{V}$, we substitute the derivative at the midpoint $(\partial \mathcal{V}/\partial \boldsymbol{q})_{n+\frac{1}{2}}$ by the approximation $(\partial \mathcal{V}/\partial \boldsymbol{q})^*_{n+\frac{1}{2}}$ (*discrete directional derivative*[6]) that satisfies the next condition:

$$(\boldsymbol{q}_{n+1} - \boldsymbol{q}_n)^T \left.\frac{\partial \mathcal{V}}{\partial \boldsymbol{q}}\right|^*_{n+\frac{1}{2}} = \mathcal{V}_{n+1} - \mathcal{V}_n \tag{18}$$

In the constraint forces term we use again the concept of *discrete directional derivative* where now the Jacobian matrix of constraints $\boldsymbol{B}_{n+\frac{1}{2}}$ is replaced by the approximation $\boldsymbol{B}^*_{n+\frac{1}{2}}$ in order to satisfy

$$(\boldsymbol{\Phi}_{n+1} - \boldsymbol{\Phi}_n) = \boldsymbol{B}^*_{n+\frac{1}{2}}(\boldsymbol{q}_{n+1} - \boldsymbol{q}_n) \tag{19}$$

With this condition,

$$(\boldsymbol{q}_{n+1} - \boldsymbol{q}_n)^T \boldsymbol{B}^{*T}_{n+\frac{1}{2}} \boldsymbol{\lambda}_{n+\frac{1}{2}} = (\boldsymbol{\Phi}_{n+1} - \boldsymbol{\Phi}_n) \boldsymbol{\lambda}_{n+\frac{1}{2}} \tag{20}$$

The configuration at time t_n is assumed to be compatible, $\boldsymbol{\Phi}_n = \boldsymbol{0}$. Then, forcing

$$\boldsymbol{\Phi}_{n+1} = \boldsymbol{0} \tag{21}$$

we guarantee that the work of the constraints forces is zero.

By replacing equations (16), (17), (18) and (19) into equation (15) we may see that the total energy change of the system over a time step results

$$\mathcal{E}_{n+1} - \mathcal{E}_n = \mathcal{K}_{n+1} - \mathcal{K}_n + \mathcal{V}_{n+1} - \mathcal{V}_n = 0 \tag{22}$$

Therefore, the scheme formed by the equation set (14) preserves the total energy of the system if (18), (19) and (21) are satisfied.

4.2 Numerical examples

The energy preserving scheme is applied to the four test cases. We observe in Figures 4 and 5 that the displacements and velocities responses computed by the energy preserving scheme are correct in the two first test cases a and b, with an exact conservation of the total energy of the system (Figure 6). The non-stiff double pendulum (test case c) is also correctly solved (Figure 7). Finally, for the stiff double pendulum (test case d), although energy is exactly preserved, the ill-conditioned mass matrix generates large spurious oscillations in the numercial response, which mask the response (Figure 8).
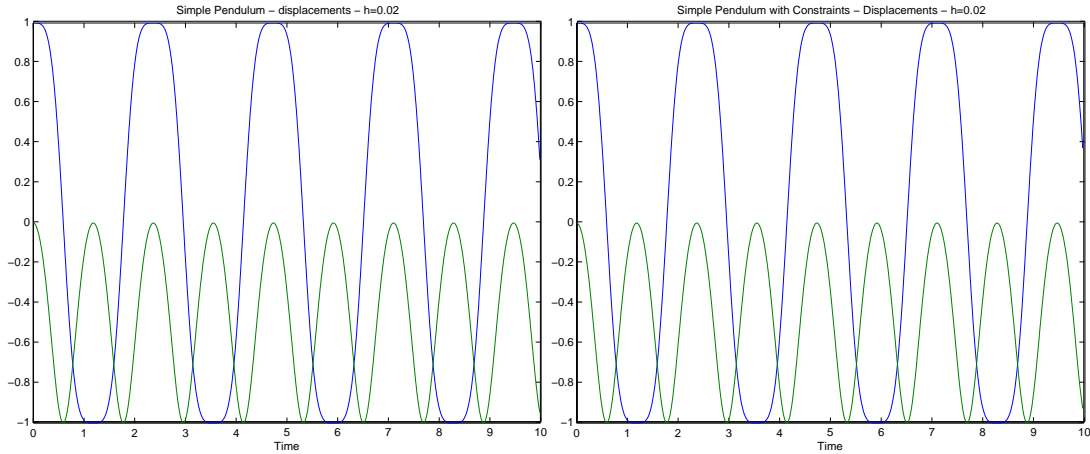
Figure 4: Simple pendulum: displacement responses for test case a (unconstrained) and test case b (constrained) in cartesian coordinates.
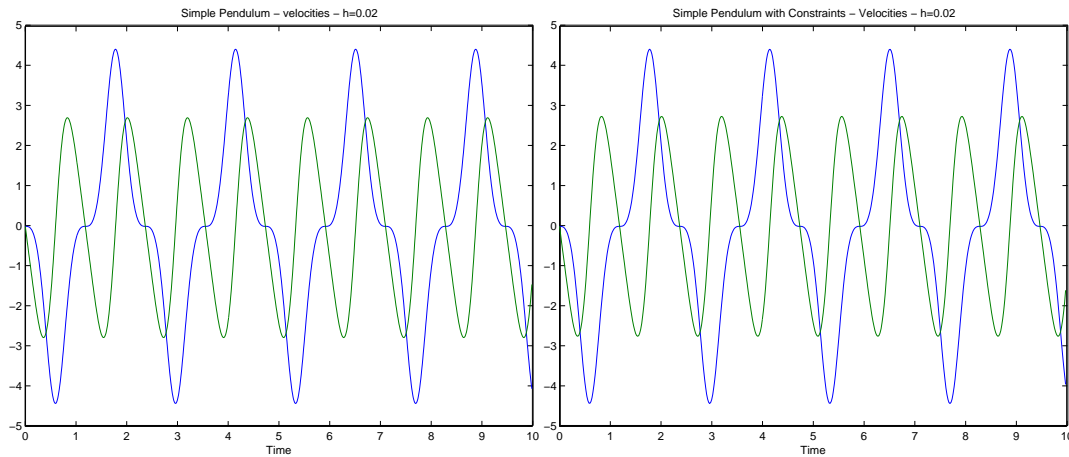

Figure 5: Simple pendulum: velocity responses for test case a (unconstrained) and test case b (constrained) in cartesian coordinates.

4.3 Conclusions

In this section a time integration scheme based on Time Continuous Galerkin Approximation with independent interpolation of displacements and velocities was introduced. A discretization process was developed for elastic and inertial forces that preserves at the discrete solution level the total mechanical energy of the system. The discretized constrained forces guarantees the exact satisfaction of nonlinear constraints and the vanishing of the work performed by the constraint forces. The Energy Preserving Scheme provides unconditional stability for nonlinear multibody systems. However, it lacks the high-frequency numerical dissipation required to tackle realistic engineering problems.
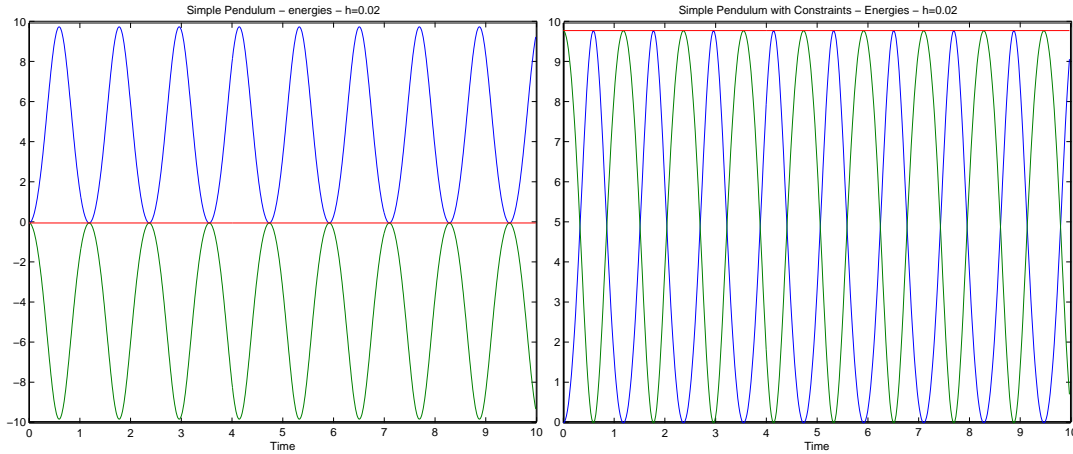
Figure 6: Simple pendulum: kinetic (blue line), potential (green line) and total energy (red line) for test case a (unconstrained) and test case b (constrained).
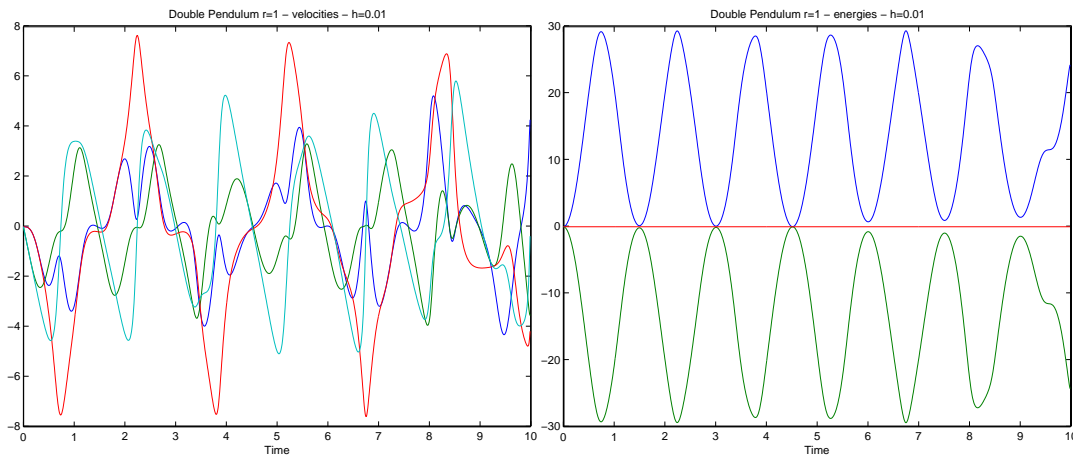

Figure 7: Double pendulum: time responses for velocities in cartesian coordinates and kinetic (blue line), potential (green line) and total energy (red line) for $m_1 = m_2 = 1$ (test case c).

5   TIME DISCONTINUOUS GALERKIN APPROXIMATION

In order to annihilate the spurious high frequency oscillations that arise in flexible problems or in rigid problems with ill- conditioned mass, we will construct in this section a new scheme that provide bounds on the algorithmic total energy over a typical time step $[t_n, t_{n+1}]$ and at the same time introduces dissipation in the high frequency regime. For this purpose we will use the Time Discontinuous Galerkin approximation, a natural way to arrive to a set of discrete equations of an algorithmic total energy dissipative scheme.[3]

Discontinuities on displacements and velocity fields q and v at the initial time t_n are allowed. A contribution taking into account the value of these discontinuities will appear in the weighted residual expressions. An additional state at time $t_j = \lim_{\varepsilon \to 0}(t_n + \varepsilon)$ is added and the following
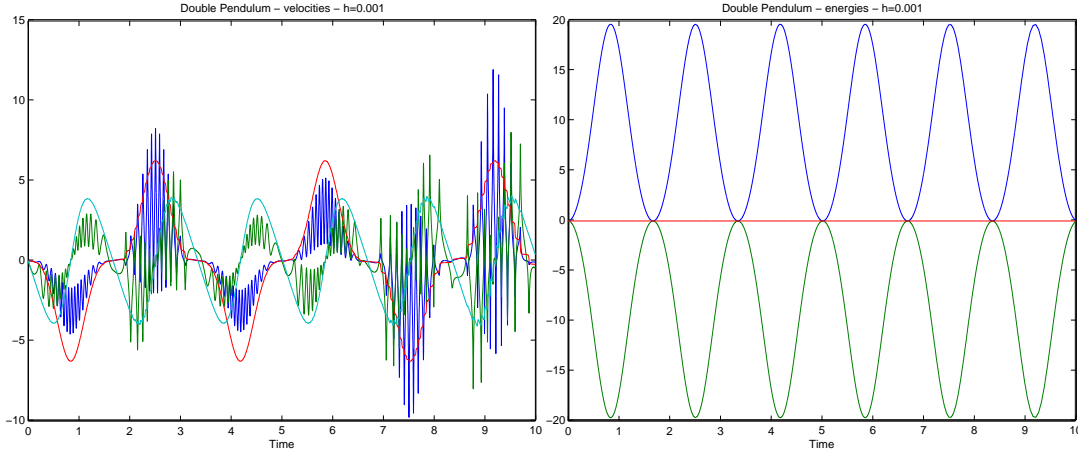
Figure 8: Double pendulum: time responses for velocities in cartesian coordinates and kinetic (blue line), potential (green line) and total energy (red line) for $m_1 = 0.005$ and $m_2 = 1$ (test case d)
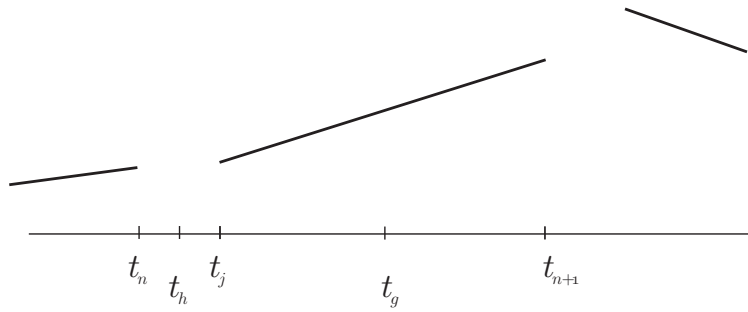

Figure 9: Discontinuous Galerkin approximation of displacements and velocities

averaged quantities at the middle points are defined:

$$(\cdot)_g = \frac{1}{2}\left((\cdot)_{n+1} + (\cdot)_j\right) \qquad (\cdot)_h = \frac{1}{2}\left((\cdot)_j + (\cdot)_n\right) \qquad (23)$$

The scheme moves forward from the initial to the final time through two coupled steps, one from t_n to t_j and other from t_j to t_{n+1}.

5.1   Energy decaying scheme without control of the amount of the dissipated energy

5.1.1   Discretization of the equation of motion

The discontinuous Galerkin approximation of the equations of motion (12) writes:

$$
\frac{h}{2}\int_{-1}^{1}\mathcal{W}_1(\tau)\left[\dot{\boldsymbol{q}} - \boldsymbol{L}^{-1}\boldsymbol{v}\right]d\tau +
$$

$$
\frac{h}{2}\int_{-1}^{1}\mathcal{W}_2(\tau)\left[\boldsymbol{M}\dot{\boldsymbol{v}} + \boldsymbol{L}^{-T}\boldsymbol{G}\dot{\boldsymbol{q}} + \boldsymbol{L}^{-T}\frac{\partial\mathcal{V}}{\partial\boldsymbol{q}} + \boldsymbol{L}^{-T}\boldsymbol{B}^T\boldsymbol{\lambda}\right]d\tau +
$$

$$
\mathcal{W}_1(-1)(\boldsymbol{q}_j - \boldsymbol{q}_n) + \mathcal{W}_2(-1)\left[\boldsymbol{M}(\boldsymbol{v}_j - \boldsymbol{v}_n) + \boldsymbol{L}^{-T}\boldsymbol{G}_h(\boldsymbol{q}_j - \boldsymbol{q}_n)\right] = \boldsymbol{0} \quad (24)
$$

where the test function are

$$
\mathcal{W}_1(\tau) = A_1 + B_1\tau \qquad \mathcal{W}_2(\tau) = A_2 + B_2\tau \tag{25}
$$

Displacements and velocities are linearly interpolated over the time step $[t_j, t_{n+1}]$:

$$
\begin{aligned}
\boldsymbol{q} &= \frac{\boldsymbol{q}_j(1-\tau) + \boldsymbol{q}_{n+1}(1+\tau)}{2} & \dot{\boldsymbol{q}} &= \frac{(\boldsymbol{q}_{n+1} - \boldsymbol{q}_j)}{h} \\
\boldsymbol{v} &= \frac{\boldsymbol{v}_j(1-\tau) + \boldsymbol{v}_{n+1}(1+\tau)}{2} & \dot{\boldsymbol{v}} &= \frac{(\boldsymbol{v}_{n+1} - \boldsymbol{v}_j)}{h}
\end{aligned} \tag{26}
$$

Internal and constraint forces are similarly interpolated, by grouping the contributions at the midpoint g:

$$
\begin{aligned}
\frac{\partial\mathcal{V}}{\partial\boldsymbol{q}} &= \left.\frac{\partial\mathcal{V}}{\partial\boldsymbol{q}}\right|_g + \frac{\tau}{2}\left(\left.\frac{\partial\mathcal{V}}{\partial\boldsymbol{q}}\right|_{n+1} - \left.\frac{\partial\mathcal{V}}{\partial\boldsymbol{q}}\right|_j\right) \\
\boldsymbol{B}^T\boldsymbol{\lambda} &= \boldsymbol{B}_g^T\boldsymbol{\lambda}_g + \frac{\tau}{2}\left[\boldsymbol{B}_{n+1}^T\boldsymbol{\lambda}_{n+1} - \boldsymbol{B}_j^T\boldsymbol{\lambda}_j\right]
\end{aligned} \tag{27}
$$

By taking independent variations on the parameters A_1, A_2, B_1 and B_2 we obtain the following discrete equation system, which is solved in an iterative form to obtain $\boldsymbol{q}_{n+1}$, $\boldsymbol{q}_j$, $\boldsymbol{v}_{n+1}$, $\boldsymbol{v}_j$, $\boldsymbol{\lambda}_g$

and $\boldsymbol{\lambda}_j$

$$
\begin{cases}
\dfrac{1}{h}\boldsymbol{L}^T\boldsymbol{M}\left(\boldsymbol{v}_{n+1}-\boldsymbol{v}_n\right)+\left.\dfrac{\partial\mathcal{V}}{\partial\boldsymbol{q}}\right|_g+\boldsymbol{B}_g^T\boldsymbol{\lambda}_g+\dfrac{1}{h}\boldsymbol{G}_m(\boldsymbol{q}_{n+1}-\boldsymbol{q}_n)=\boldsymbol{0}\\[2mm]
\dfrac{1}{h}\boldsymbol{L}^T\boldsymbol{M}\left(\boldsymbol{v}_j-\boldsymbol{v}_n\right)-\dfrac{1}{3}\left[\left.\dfrac{\partial\mathcal{V}}{\partial\boldsymbol{q}}\right|_g-\left.\dfrac{\partial\mathcal{V}}{\partial\boldsymbol{q}}\right|_h\right]+\dfrac{1}{6}\left[\left.\dfrac{\partial\mathcal{V}}{\partial\boldsymbol{q}}\right|_j-\left.\dfrac{\partial\mathcal{V}}{\partial\boldsymbol{q}}\right|_n\right]-\\[2mm]
\qquad\qquad\qquad\dfrac{1}{3}\left(\boldsymbol{B}_g^T\boldsymbol{\lambda}_g-\boldsymbol{B}_h^T\boldsymbol{\lambda}_j\right)+\dfrac{1}{h}\boldsymbol{G}_h(\boldsymbol{q}_j-\boldsymbol{q}_n)=\boldsymbol{0}\\[2mm]
\dfrac{1}{h}\boldsymbol{L}(\boldsymbol{q}_{n+1}-\boldsymbol{q}_n)-\dfrac{1}{2}(\boldsymbol{v}_{n+1}-\boldsymbol{v}_j)=\boldsymbol{0}\\[2mm]
\dfrac{1}{h}\boldsymbol{L}(\boldsymbol{q}_j-\boldsymbol{q}_n)+\dfrac{1}{6}(\boldsymbol{v}_{n+1}-\boldsymbol{v}_j)=\boldsymbol{0}\\[2mm]
\boldsymbol{\Phi}_j=\boldsymbol{0}\\[2mm]
\boldsymbol{\Phi}_{n+1}=\boldsymbol{0}
\end{cases}
\tag{28}
$$

We have used the fact that $\boldsymbol{L}$ is constant for the adopted rotation parametrization and where we made the approximation :

$$
\boldsymbol{G}_g(\boldsymbol{q}_{n+1}-\boldsymbol{q}_j)+\boldsymbol{G}_h(\boldsymbol{q}_j-\boldsymbol{q}_n)\simeq\boldsymbol{G}_m(\boldsymbol{q}_{n+1}-\boldsymbol{q}_n)
\tag{29}
$$

with:

$$
\boldsymbol{G}_m=\boldsymbol{G}_m(\boldsymbol{H}_m);\quad\boldsymbol{H}_m=\frac{1}{2}(\boldsymbol{H}_n+\boldsymbol{H}_{n+1})=\frac{1}{2}\boldsymbol{J}(\boldsymbol{\Omega}_n+\boldsymbol{\Omega}_{n+1})
\tag{30}
$$

5.1.2 Energy decay in the discrete scheme

If we multiply (28-a) by the displacements jump $(\boldsymbol{q}_{n+1}-\boldsymbol{q}_n)$ and (28-b) by $(\boldsymbol{q}_j-\boldsymbol{q}_n)$, we have:

$$
\frac{1}{h}(\boldsymbol{q}_{n+1}-\boldsymbol{q}_n)^T\boldsymbol{L}^T\boldsymbol{M}\left(\boldsymbol{v}_{n+1}-\boldsymbol{v}_n\right)+(\boldsymbol{q}_{n+1}-\boldsymbol{q}_n)^T\left.\frac{\partial\mathcal{V}}{\partial\boldsymbol{q}}\right|_g+
$$
$$
(\boldsymbol{q}_{n+1}-\boldsymbol{q}_n)^T\boldsymbol{B}_g^T\boldsymbol{\lambda}_g+\frac{1}{h}(\boldsymbol{q}_{n+1}-\boldsymbol{q}_n)^T\boldsymbol{G}_m(\boldsymbol{q}_{n+1}-\boldsymbol{q}_n)=0
$$

$$
\frac{1}{h}(\boldsymbol{q}_j-\boldsymbol{q}_n)^T\boldsymbol{L}^T\boldsymbol{M}\left(\boldsymbol{v}_j-\boldsymbol{v}_n\right)-\frac{1}{3}(\boldsymbol{q}_j-\boldsymbol{q}_n)^T\left[\left.\frac{\partial\mathcal{V}}{\partial\boldsymbol{q}}\right|_g-\left.\frac{\partial\mathcal{V}}{\partial\boldsymbol{q}}\right|_h\right]+
$$
$$
\frac{1}{6}(\boldsymbol{q}_j-\boldsymbol{q}_n)^T\left[\left.\frac{\partial\mathcal{V}}{\partial\boldsymbol{q}}\right|_j-\left.\frac{\partial\mathcal{V}}{\partial\boldsymbol{q}}\right|_n\right]-\frac{1}{3}(\boldsymbol{q}_j-\boldsymbol{q}_n)^T\left(\boldsymbol{B}_g^T\boldsymbol{\lambda}_g-\boldsymbol{B}_h^T\boldsymbol{\lambda}_j\right)+
$$
$$
\frac{1}{h}(\boldsymbol{q}_j-\boldsymbol{q}_n)^T\boldsymbol{G}_h(\boldsymbol{q}_j-\boldsymbol{q}_n)=0
\tag{31}
$$

By using the displacements-velocities relationships (28-c) and (28-d) and by linearly combining equations (31-a) and (31-b) we arrive at:

$$
\frac{1}{2}(\boldsymbol{v}_{n+1} + \boldsymbol{v}_j)^T \boldsymbol{M}(\boldsymbol{v}_{n+1} - \boldsymbol{v}_n) - \frac{1}{2}(\boldsymbol{v}_{n+1} - \boldsymbol{v}_j)^T \boldsymbol{M}(\boldsymbol{v}_j - \boldsymbol{v}_n)+
$$
$$
(\boldsymbol{q}_{n+1} - \boldsymbol{q}_j)^T \left.\frac{\partial \mathcal{V}}{\partial \boldsymbol{q}}\right|_g + (\boldsymbol{q}_j - \boldsymbol{q}_n)^T \left.\frac{\partial \mathcal{V}}{\partial \boldsymbol{q}}\right|_h + \frac{1}{2}(\boldsymbol{q}_j - \boldsymbol{q}_n)^T \left[\left.\frac{\partial \mathcal{V}}{\partial \boldsymbol{q}}\right|_j - \left.\frac{\partial \mathcal{V}}{\partial \boldsymbol{q}}\right|_n\right]+
$$
$$
(\boldsymbol{q}_{n+1} - \boldsymbol{q}_n)^T \boldsymbol{B}_g^T \boldsymbol{\lambda}_g - (\boldsymbol{q}_j - \boldsymbol{q}_n)^T (\boldsymbol{B}_g^T \boldsymbol{\lambda}_g - \boldsymbol{B}_h^T \boldsymbol{\lambda}_j)+
$$
$$
(\boldsymbol{q}_{n+1} - \boldsymbol{q}_n)^T \frac{1}{h} \boldsymbol{G}_m (\boldsymbol{q}_{n+1} - \boldsymbol{q}_n) + (\boldsymbol{q}_j - \boldsymbol{q}_n)^T \frac{1}{h} \boldsymbol{G}_h (\boldsymbol{q}_j - \boldsymbol{q}_n) = \boldsymbol{0} \quad (32)
$$

After some algebra, it can be shown that the two first terms are equal to the sum of the kinetic energy jump over the time step $[t_n, t_{n+1}]$ plus a positive term $\mathcal{K}_{nj}$ which we call *kinetic energy of the jump*:

$$
\frac{1}{2}(\boldsymbol{v}_{n+1} + \boldsymbol{v}_n)^T \boldsymbol{M}(\boldsymbol{v}_{n+1} - \boldsymbol{v}_j) - \frac{1}{2}(\boldsymbol{v}_{n+1} - \boldsymbol{v}_j)^T \boldsymbol{M}(\boldsymbol{v}_j - \boldsymbol{v}_n) = \mathcal{K}_{n+1} - \mathcal{K}_n + \mathcal{K}_{nj} \quad (33)
$$

where the *kinetic energy of the jump* is defined as

$$
\mathcal{K}_{nj} = \frac{1}{2}(\boldsymbol{v}_j - \boldsymbol{v}_n)^T \boldsymbol{M}(\boldsymbol{v}_j - \boldsymbol{v}_n) \geqq 0 \quad (34)
$$

Once again, we replace the midpoint elastic forces $(\partial \mathcal{V}/\partial \boldsymbol{q})_g$ and $(\partial \mathcal{V}/\partial \boldsymbol{q})_h$ by their *discrete directional derivative* counterparts, giving the jump of potential energy over the time step:

$$
(\boldsymbol{q}_{n+1} - \boldsymbol{q}_j)^T \left.\frac{\partial \mathcal{V}}{\partial \boldsymbol{q}}\right|_g^* + (\boldsymbol{q}_j - \boldsymbol{q}_n)^T \left.\frac{\partial \mathcal{V}}{\partial \boldsymbol{q}}\right|_h^* = \mathcal{V}_{n+1} - \mathcal{V}_j + \mathcal{V}_j - \mathcal{V}_n = \mathcal{V}_{n+1} - \mathcal{V}_n \quad (35)
$$

The third term involving derivatives of potential energy will be called *potential energy of the jump* and is positive for convex potential energy functions:

$$
\mathcal{V}_{nj} = \frac{1}{2}(\boldsymbol{q}_j - \boldsymbol{q}_n)^T \left[\left.\frac{\partial \mathcal{V}}{\partial \boldsymbol{q}}\right|_j - \left.\frac{\partial \mathcal{V}}{\partial \boldsymbol{q}}\right|_n\right] \geqq 0 \quad (36)
$$

For the constraint forces we approximate the matrices $\boldsymbol{B}_g$ and $\boldsymbol{B}_h$ with $\boldsymbol{B}_g^*$ and $\boldsymbol{B}_h^*$, using again the concept of *discrete directional derivative* in such a way that

$$
\boldsymbol{B}_g^*(\boldsymbol{q}_{n+1} - \boldsymbol{q}_j) = \boldsymbol{\Phi}_{n+1} - \boldsymbol{\Phi}_j; \quad \boldsymbol{B}_h^*(\boldsymbol{q}_j - \boldsymbol{q}_n) = \boldsymbol{\Phi}_j - \boldsymbol{\Phi}_n \quad (37)
$$

Then we have:

$$
(\boldsymbol{q}_{n+1} - \boldsymbol{q}_n)^T \boldsymbol{B}_g^{*T} \boldsymbol{\lambda}_g - (\boldsymbol{q}_j - \boldsymbol{q}_n)^T (\boldsymbol{B}_g^{*T} \boldsymbol{\lambda}_g - \boldsymbol{B}_h^{*T} \boldsymbol{\lambda}_j) = (\boldsymbol{\Phi}_{n+1} - \boldsymbol{\Phi}_j)^T \boldsymbol{\lambda}_g + (\boldsymbol{\Phi}_j - \boldsymbol{\Phi}_n)^T \boldsymbol{\lambda}_j \quad (38)
$$

The configuration at time t_n is assumed to be compatible, $\boldsymbol{\Phi}_n = \boldsymbol{0}$. Then if we enforce

$$\boldsymbol{\Phi}_j = \boldsymbol{0} \qquad \text{and} \qquad \boldsymbol{\Phi}_{n+1} = \boldsymbol{0} \tag{39}$$

this implies that the work of the constraints forces vanishes.
Finally for the last two terms we have that

$$(\boldsymbol{q}_{n+1} - \boldsymbol{q}_n)^T \frac{1}{h} \boldsymbol{G}_m (\boldsymbol{q}_{n+1} - \boldsymbol{q}_n) = 0$$

$$(\boldsymbol{q}_j - \boldsymbol{q}_n)^T \frac{1}{h} \boldsymbol{G}_h (\boldsymbol{q}_j - \boldsymbol{q}_n) = 0 \tag{40}$$

because of the skew-symmetry of $\boldsymbol{G}_m$ and $\boldsymbol{G}_h$.
By replacing (33), (34), (35), (36), (37) and (40) in (32) we may see that the change of the total energy of the system becomes

$$\mathcal{E}_{n+1} - \mathcal{E}_n = \mathcal{K}_{n+1} - \mathcal{K}_n + \mathcal{V}_{n+1} - \mathcal{V}_n + c^2 \tag{41}$$

where the quadratic term is the *total energy of the jump*

$$c^2 = \mathcal{E}_{nj} = \mathcal{K}_{nj} + \mathcal{V}_{nj} \geqq 0 \tag{42}$$

Finally, we have that

$$\mathcal{E}_{n+1} = \mathcal{E}_n - c^2 \longrightarrow \mathcal{E}_{n+1} \leqq \mathcal{E}_n \tag{43}$$

that is the scheme proposed by the set of equations (28) implies the inequality (43), which guarantees the decay of the total energy of the system if (35), (36), (37) and (39) are satisfied.

5.1.3 Numerical examples

We will solve now the test examples using the proposed energy decaying scheme. We can observe that the numerical oscillations disappear in the displacements and velocities time responses for the double pendulum with ill conditioned mass matrix (Figure 10). However, Figure 11 shows that the scheme dissipates too much energy. For the simple pendulum the responses are plotted in Figures 12 and 13. We observe that for the case of the constrained model, the energy dissipation is again excessive.

5.1.4 Conclusions

We developed a time integration scheme based on Time Discontinuous Galerkin approximation with independent interpolation of displacements and velocities. The scheme is closely related to the Energy Preserving scheme and it implies a discrete energy decay statement. The discretization process for the constraint forces is left unchanged, that is the work they perform vanishes exactly and constraints are exactly satisfied. This procedure provides nonlinear unconditional stability and high frequency numerical dissipation. We note that there is no control on the amount of dissipated energy. We note also that, although unconstrained problems are solved correctly with a small amount of dissipation, the computed solutions for nonlinear constrained problems present an excessive amount of energy dissipation.
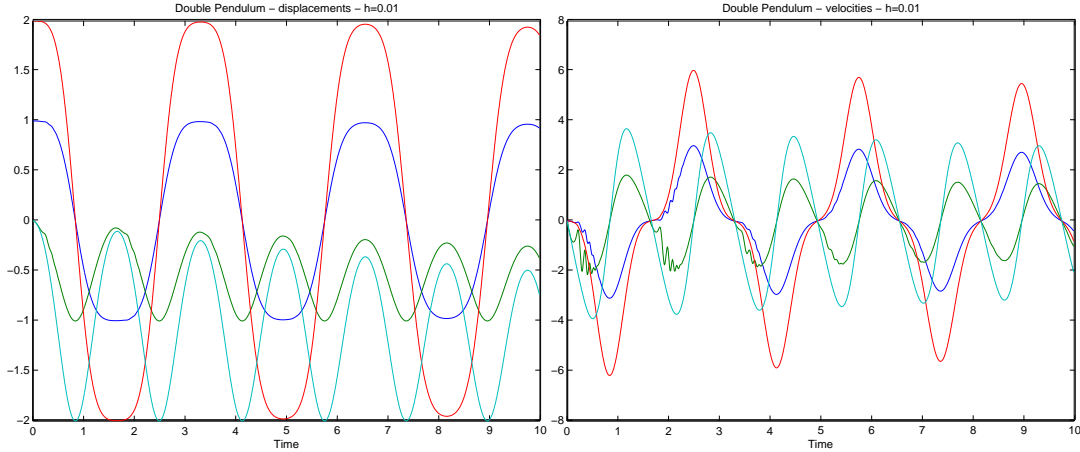
Figure 10: Double pendulum: time responses for displacements and velocities in cartesian coordinates for $m_1 = 0.005$, $m_2 = 1$ (test case d)
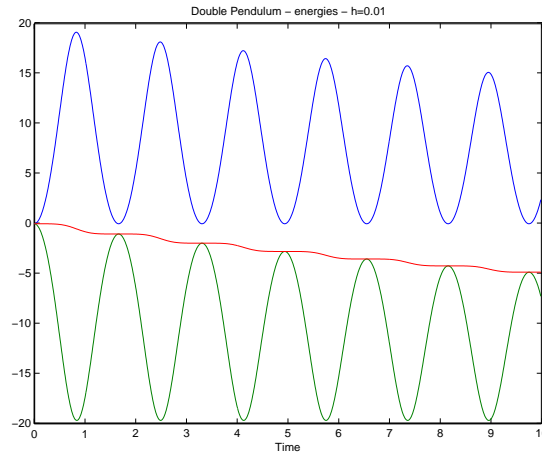

Figure 11: Double pendulum: time responses for kinetic (blue line), potential (green line) and total energy (red line) for $m_1 = 0.005$ and $m_2 = 1$(test case d).

5.2 Energy decaying scheme with control of dissipated energy

The algorithm proposed in the previous section is now extended to a numerically dissipative scheme with control of dissipation. The procedure is exactly the same as before but the expressions of the interpolated displacements, velocities and internal forces are now:

$$
\begin{aligned}
\boldsymbol{q} &= \frac{(\boldsymbol{q}_j + \boldsymbol{q}_{n+1})}{2} + \tau \frac{(\boldsymbol{q}_{n+1} - \alpha \boldsymbol{q}_j - (1-\alpha)\boldsymbol{q}_n)}{2} & \dot{\boldsymbol{q}} &= \frac{(\boldsymbol{q}_{n+1} - \boldsymbol{q}_j)}{h} \\
\boldsymbol{v} &= \frac{(\boldsymbol{v}_j + \boldsymbol{v}_{n+1})}{2} + \tau \frac{(\boldsymbol{v}_{n+1} - \alpha \boldsymbol{v}_j - (1-\alpha)\boldsymbol{v}_n)}{2} & \dot{\boldsymbol{v}} &= \frac{(\boldsymbol{v}_{n+1} - \boldsymbol{v}_j)}{h}
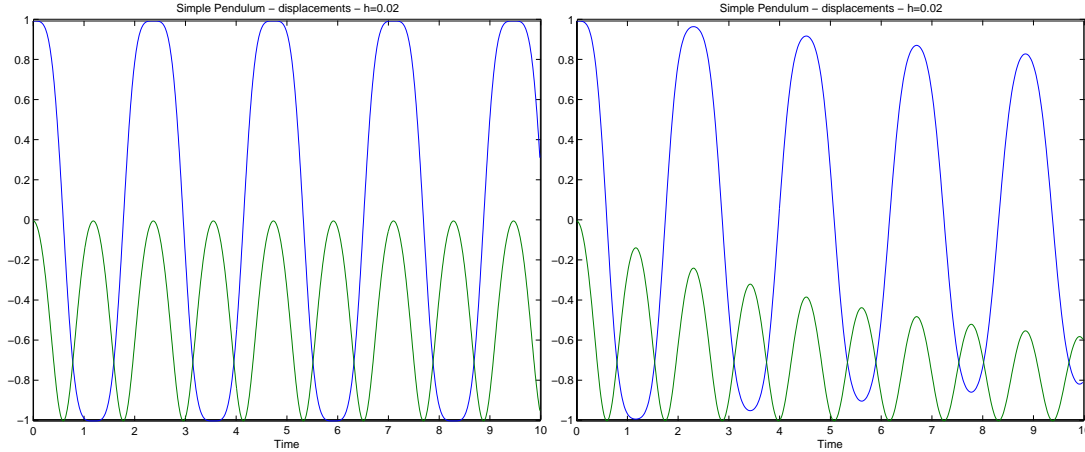\end{aligned}
\tag{44}
$$

Figure 12: Simple pendulum: displacements for test case a (unconstrained) and test case b (constrained) in cartesian coordinates.
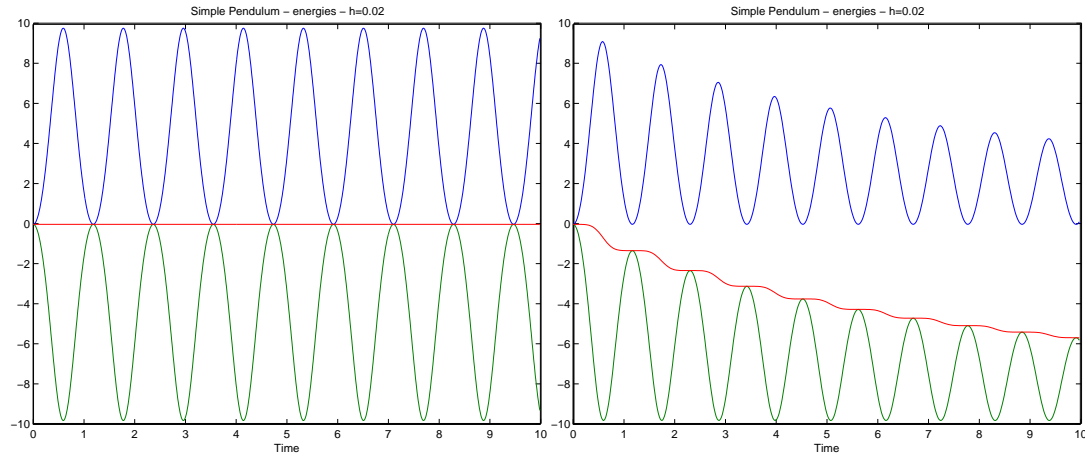

Figure 13: Simple pendulum: kinetic (blue line), potential (green line) and total energy (red line) for test case a (unconstrained) and test case b (constrained).

$$\frac{\partial \mathcal{V}}{\partial \boldsymbol{q}} = \left.\frac{\partial \mathcal{V}}{\partial \boldsymbol{q}}\right|_g + \frac{\tau}{2}\left[\left.\frac{\partial \mathcal{V}}{\partial \boldsymbol{q}}\right|_{n+1} - \alpha \left.\frac{\partial \mathcal{V}}{\partial \boldsymbol{q}}\right|_j - (1-\alpha)\left.\frac{\partial \mathcal{V}}{\partial \boldsymbol{q}}\right|_n\right] \tag{45}$$

where the algorithmic parameter $\alpha \in [0,1]$ controls the amount of dissipation. On the other hand, the forces of constraint are interpolated as in the previous scheme:

$$\boldsymbol{B}^T\boldsymbol{\lambda} = \boldsymbol{B}_g^T\boldsymbol{\lambda}_g + \frac{\tau}{2}\left(\boldsymbol{B}_{n+1}^T\boldsymbol{\lambda}_{n+1} - \boldsymbol{B}_j^T\boldsymbol{\lambda}_j\right) \tag{46}$$

The weight functions are the same used for the previous scheme.

5.2.1 Discretization of the equation of motion

A weighted residual expression of the equations of motion (12) is formed, as in the previous scheme, and after integration, the TDG discrete form of the equations of motion writes:

$$
\begin{cases}
\dfrac{1}{h}\boldsymbol{L}^T\boldsymbol{M}(\boldsymbol{v}_{n+1}-\boldsymbol{v}_n)+\dfrac{1}{h}\boldsymbol{G}_m(\boldsymbol{q}_{n+1}-\boldsymbol{q}_n)+\left.\dfrac{\partial\mathcal{V}}{\partial\boldsymbol{q}}\right|_g+(\boldsymbol{B}^T\boldsymbol{\lambda})_g=\boldsymbol{0}\\[2ex]
\dfrac{1}{h}\boldsymbol{L}^T\boldsymbol{M}(\boldsymbol{v}_j-\boldsymbol{v}_n)+\dfrac{1}{h}\boldsymbol{G}_h(\boldsymbol{q}_j-\boldsymbol{q}_n)-\dfrac{1}{3}\left[\left.\dfrac{\partial\mathcal{V}}{\partial\boldsymbol{q}}\right|_g-\left.\dfrac{\partial\mathcal{V}}{\partial\boldsymbol{q}}\right|_h\right]\\[2ex]
\qquad\qquad +\dfrac{1}{6}\alpha\left[\left.\dfrac{\partial\mathcal{V}}{\partial\boldsymbol{q}}\right|_j-\left.\dfrac{\partial\mathcal{V}}{\partial\boldsymbol{q}}\right|_n\right]-\dfrac{1}{3}(\boldsymbol{B}_g^T\boldsymbol{\lambda}_g-\boldsymbol{B}_h^T\boldsymbol{\lambda}_j)=\boldsymbol{0}\\[2ex]
\boldsymbol{L}\dfrac{1}{h}(\boldsymbol{q}_{n+1}-\boldsymbol{q}_n)=\dfrac{1}{2}(\boldsymbol{v}_j+\boldsymbol{v}_{n+1})\\[2ex]
\boldsymbol{L}\dfrac{1}{h}(\boldsymbol{q}_j-\boldsymbol{q}_n)=-\dfrac{1}{6}\left[\boldsymbol{v}_{n+1}-\alpha\boldsymbol{v}_j+(\alpha-1)\boldsymbol{v}_n\right]\\[2ex]
\boldsymbol{\Phi}_j=\boldsymbol{0}\\[1ex]
\boldsymbol{\Phi}_{n+1}=\boldsymbol{0}
\end{cases}
\tag{47}
$$

with $0\le\alpha\le1$.

5.2.2 Energy decay in the discrete scheme

Now we will prove the decay of the energy for this scheme. For this purpose we multiply Eq. (47-a) by $(\boldsymbol{q}_{n+1}-\boldsymbol{q}_n)^T$ and Eq. (47-b) by $(\boldsymbol{q}_j-\boldsymbol{q}_n)^T$ and get

$$
\dfrac{1}{h}(\boldsymbol{q}_{n+1}-\boldsymbol{q}_n)^T\boldsymbol{L}^T\boldsymbol{M}(\boldsymbol{v}_{n+1}-\boldsymbol{v}_n)+\dfrac{1}{h}(\boldsymbol{q}_{n+1}-\boldsymbol{q}_n)^T\boldsymbol{G}_m(\boldsymbol{q}_{n+1}-\boldsymbol{q}_n)+
$$
$$
(\boldsymbol{q}_{n+1}-\boldsymbol{q}_n)^T\left.\dfrac{\partial\mathcal{V}}{\partial\boldsymbol{q}}\right|_g+(\boldsymbol{q}_{n+1}-\boldsymbol{q}_n)^T(\boldsymbol{B}^T\boldsymbol{\lambda})_g=0 \tag{48}
$$

$$
\dfrac{1}{h}(\boldsymbol{q}_j-\boldsymbol{q}_n)^T\boldsymbol{L}^T\boldsymbol{M}(\boldsymbol{v}_j-\boldsymbol{v}_n)+\dfrac{1}{h}(\boldsymbol{q}_j-\boldsymbol{q}_n)^T\boldsymbol{G}_h(\boldsymbol{q}_j-\boldsymbol{q}_n)-(\boldsymbol{q}_j-\boldsymbol{q}_n)^T\dfrac{1}{3}\left[\left.\dfrac{\partial\mathcal{V}}{\partial\boldsymbol{q}}\right|_g-\left.\dfrac{\partial\mathcal{V}}{\partial\boldsymbol{q}}\right|_h\right]
$$
$$
+(\boldsymbol{q}_j-\boldsymbol{q}_n)^T\dfrac{1}{6}\alpha\left[\left.\dfrac{\partial\mathcal{V}}{\partial\boldsymbol{q}}\right|_j-\left.\dfrac{\partial\mathcal{V}}{\partial\boldsymbol{q}}\right|_n\right]-(\boldsymbol{q}_j-\boldsymbol{q}_n)^T\dfrac{1}{3}(\boldsymbol{B}_g^T\boldsymbol{\lambda}-\boldsymbol{B}_h^T\boldsymbol{\lambda}_j)=0 \tag{49}
$$

Combining linearly these two last expressions we arrive at

$$\frac{1}{2}(\boldsymbol{v}_j + \boldsymbol{v}_{n+1})^T \boldsymbol{M}(\boldsymbol{v}_{n+1} - \boldsymbol{v}_n) - \frac{1}{2}\left[\boldsymbol{v}_{n+1} - \alpha\boldsymbol{v}_j + (\alpha - 1)\boldsymbol{v}_n\right]^T \boldsymbol{M}(\boldsymbol{v}_j - \boldsymbol{v}_n) +$$

$$(\boldsymbol{q}_{n+1} - \boldsymbol{q}_n)^T \left.\frac{\partial\mathcal{V}}{\partial\boldsymbol{q}}\right|_g - (\boldsymbol{q}_j - \boldsymbol{q}_n)^T\frac{1}{2}\left[\left.\frac{\partial\mathcal{V}}{\partial\boldsymbol{q}}\right|_g - \left.\frac{\partial\mathcal{V}}{\partial\boldsymbol{q}}\right|_h\right] +$$

$$- (\boldsymbol{q}_j - \boldsymbol{q}_n)^T\frac{1}{2}\alpha\left[\left.\frac{\partial\mathcal{V}}{\partial\boldsymbol{q}}\right|_j - \left.\frac{\partial\mathcal{V}}{\partial\boldsymbol{q}}\right|_n\right] + (\boldsymbol{q}_{n+1} - \boldsymbol{q}_n)^T \boldsymbol{B}_g^T\boldsymbol{\lambda}_g - (\boldsymbol{q}_j - \boldsymbol{q}_n)^T(\boldsymbol{B}_g^T\boldsymbol{\lambda}_g - \boldsymbol{B}_h^T\boldsymbol{\lambda}_j) = 0$$

(50)

where, after some algebra, we identify the terms corresponding to the kinetic energy jump $\mathcal{K}_{n+1} - \mathcal{K}_n$, and the *kinetic energy of the jump* $\mathcal{K}_{nj}$, multiplied by the factor α:

$$\frac{1}{2}(\boldsymbol{v}_j + \boldsymbol{v}_{n+1})^T \boldsymbol{M}(\boldsymbol{v}_{n+1} - \boldsymbol{v}_n) - \frac{1}{2}\left[\boldsymbol{v}_{n+1} - \alpha\boldsymbol{v}_j + (\alpha - 1)\boldsymbol{v}_n\right]^T \boldsymbol{M}(\boldsymbol{v}_j - \boldsymbol{v}_n) =$$

$$\mathcal{K}_{n+1} - \mathcal{K}_n + \alpha\mathcal{K}_{nj} = \mathcal{K}_{n+1} - \mathcal{K}_n + \alpha\mathcal{K}_{nj}$$

The expression of the *kinetic energy of the jump* is as before:

$$\mathcal{K}_{nj} = \frac{1}{2}(\boldsymbol{v}_j - \boldsymbol{v}_n)^T \boldsymbol{M}(\boldsymbol{v}_j - \boldsymbol{v}_n) \geqq 0$$

(51)

Once again, we will use the concept of the *discrete directional derivative* for the potential energy terms, to replace the expressions $(\partial\mathcal{V}/\partial\boldsymbol{q})_g$ and $(\partial\mathcal{V}/\partial\boldsymbol{q})_h$ by their discrete directional counterparts in order to verify (35).

$$(\boldsymbol{q}_{n+1} - \boldsymbol{q}_j)^T \left.\frac{\partial\mathcal{V}}{\partial\boldsymbol{q}}\right|_g^* + (\boldsymbol{q}_j - \boldsymbol{q}_n)^T \left.\frac{\partial\mathcal{V}}{\partial\boldsymbol{q}}\right|_h^* + (\boldsymbol{q}_j - \boldsymbol{q}_n)^T\frac{1}{2}\alpha\left[\left.\frac{\partial\mathcal{V}}{\partial\boldsymbol{q}}\right|_j - \left.\frac{\partial\mathcal{V}}{\partial\boldsymbol{q}}\right|_n\right] =$$

$$(\mathcal{V}_{n+1} - \mathcal{V}_j) + (\mathcal{V}_j - \mathcal{V}_n) + (\boldsymbol{q}_j - \boldsymbol{q}_n)^T\frac{1}{2}\alpha\left[\left.\frac{\partial\mathcal{V}}{\partial\boldsymbol{q}}\right|_j - \left.\frac{\partial\mathcal{V}}{\partial\boldsymbol{q}}\right|_n\right]$$

In the RHS we identify the potential energy jump over the time step $[t_n, t_{n+1}]$ plus the *potential energy of the jump*, that in order to be positive must also satisfy the local convexity expressed in (36). The constraint and gyroscopic forces are treated in the same way as in the previous section, i.e. the work done by them is null.

Finally the total energy has the expression:

$$\mathcal{E}_{n+1} - \mathcal{E}_n = \mathcal{K}_{n+1} - \mathcal{K}_n - \alpha\mathcal{K}_{nj} + \mathcal{V}_{n+1} - \mathcal{V}_n - \alpha\mathcal{V}_{nj} = 0$$

(52)

from which

$$\mathcal{E}_{n+1} = (\mathcal{K}_n + \mathcal{V}_n) - \alpha(\mathcal{K}_{nj} + \mathcal{V}_{nj}) = \mathcal{E}_n - \alpha c^2 \quad c^2 \geq 0$$

(53)

For $\alpha = 0$ we have an energy preserving scheme (note it is different from that of section 4) while for $\alpha = 1$ we have the maximum energy dissipation. Note also that we recover the energy decaying scheme presented in the previous section for $\alpha = 1$.

5.2.3 Numerical examples

We will show the results obtained for the simple and the double pendulum described in section 4.2. Figure 14 plots the simple pendulum displacements responses for the case $\alpha = 0$ for
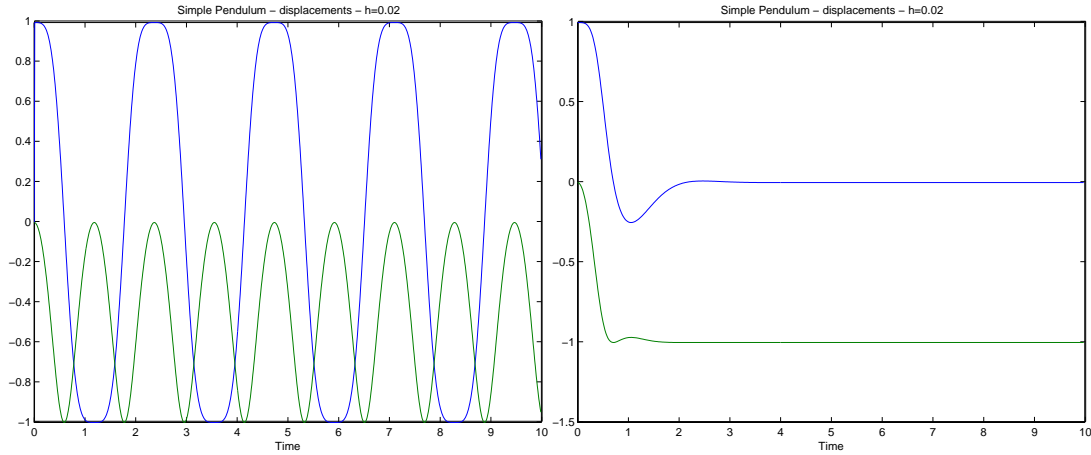

Figure 14: Simple pendulum: displacements for test case a (unconstrained) and test case b (constrained) in cartesian coordinates.
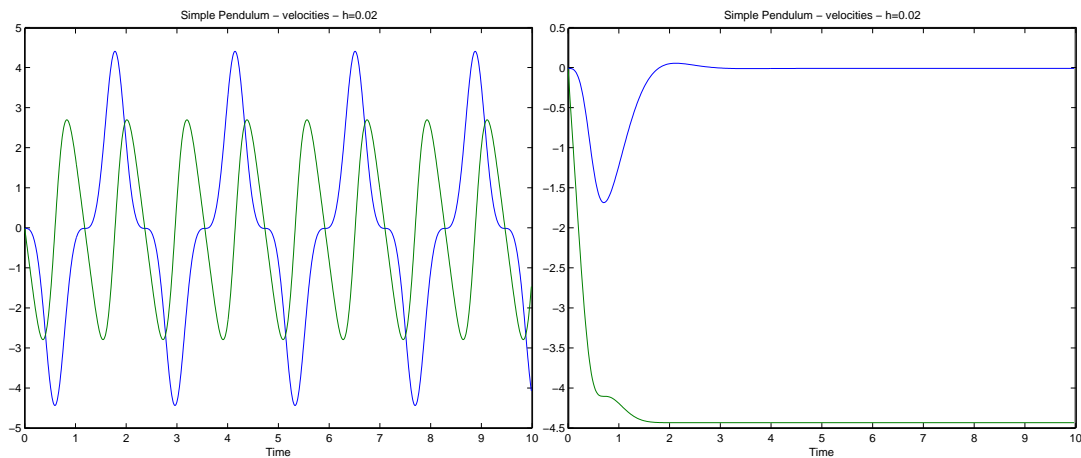

Figure 15: Simple pendulum: velocities for test case a (unconstrained) and test case b (constrained) in cartesian coordinates.

both models, a and b whereas Figure 15 displays the velocities time responses. Clearly both responses are not similar at all. We observe a locking phenomenon in the responses for the constrained model. This locking phenomenon is also observed in the responses for the double pendulum, modelled with constraints. In all cases, the total energy is perfectly preserved for the energy preserving scheme (Figure 16). Figure 17 shows the amount of dissipation changes
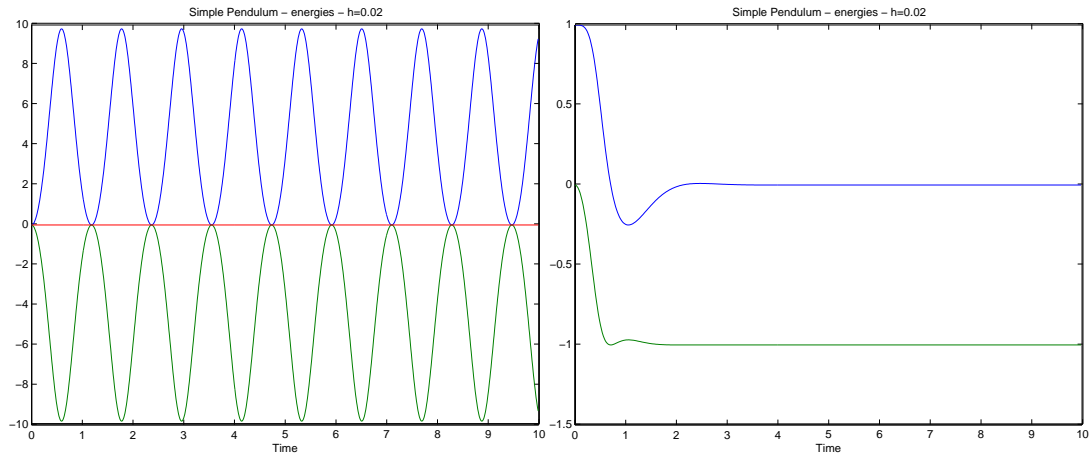
Figure 16: Simple pendulum: kinetic (blue line), potential (green line) and total energy (red line) for test case a (unconstrained) and test case b (constrained).
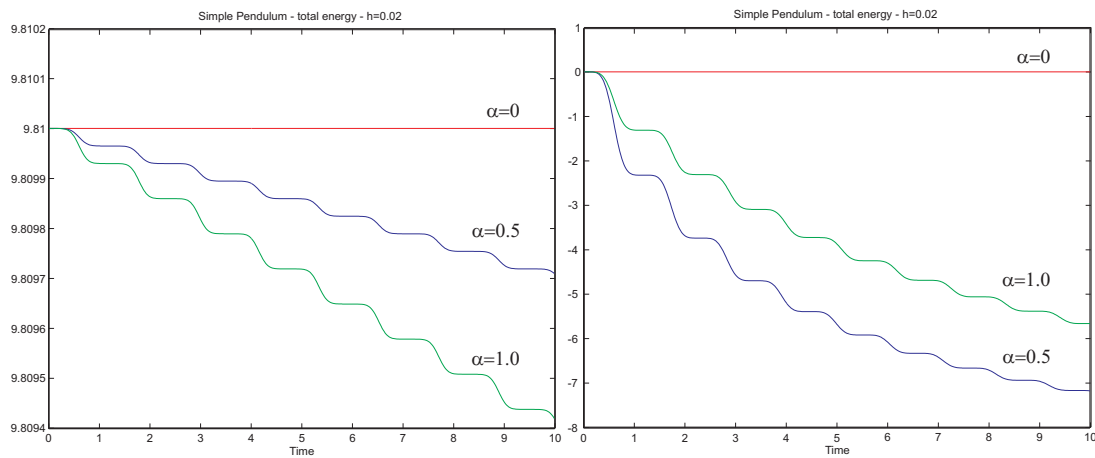

Figure 17: Simple pendulum: total energy for test case a (unconstrained) and test case b (constrained) for different values of parameter α.

for different values of the parameter α for the simple pendulum. For the constrained model we see that the greatest amount of dissipation does not coincide with the $\alpha = 1$ like in the case of unconstrained model. Moreover, the energy decays almost 10000 times more for the constrained case.

5.2.4 Conclusions

In this section we have introduced a scheme with an algorithmic control of the amount of energy dissipated. This control works well only for unconstrained problems (and also for linearly constrained cases). The amount of dissipation increases monotonously with α from 0 to 1 only for unconstrained cases. A locking phenomenon arises for constrained cases, when $\alpha = 0$ and

an excessive dissipation is reached when $\alpha \neq 0$. We attribute these problems to the independent interpolation fields of displacements and velocities.

5.3 Energy decaying scheme with velocities constraints and α and κ parameters

In order to avoid the troubles that arose with the previous scheme, we will reformulate it using the constraint stabilization technique proposed by Gear *et al*,[7] based on the reduction of the governing equations from index-3 to index-2 DAEs. The idea is to introduce a new algebraic constraint equation $\boldsymbol{B}\boldsymbol{L}^{-1}\boldsymbol{v} = \boldsymbol{0}$ where $\boldsymbol{\eta}$ is the Lagrange multiplier associated to the new constraint. If we apply the Hamilton's principle in the same way as we did in section 2, the new motion equations will result from:

$$\delta \int_{t_1}^{t_2} \left\{ \mathcal{L} - \boldsymbol{\mu}^T(\boldsymbol{v} - \boldsymbol{L}\dot{\boldsymbol{q}}) - \boldsymbol{\lambda}^T\boldsymbol{\Phi} - \boldsymbol{\eta}^T\boldsymbol{B}\boldsymbol{L}^{-1}\boldsymbol{v} \right\} dt = 0 \tag{54}$$

If we perform the variation on the variable $\boldsymbol{v}$, we get

$$\boldsymbol{\mu} = \boldsymbol{M}\boldsymbol{v} - \boldsymbol{L}^{-T}\boldsymbol{B}^T\boldsymbol{\eta} \tag{55}$$

Now introducing this expression in (54) and with the help of (3) we finally obtain:

$$\delta \int_{t_1}^{t_2} \left\{ -\frac{1}{2}\boldsymbol{v}^T\boldsymbol{M}\boldsymbol{v} - \mathcal{V}(\boldsymbol{q}) + \boldsymbol{v}^T\boldsymbol{M}\boldsymbol{L}\dot{\boldsymbol{q}} - \boldsymbol{\lambda}^T\boldsymbol{\Phi} - \boldsymbol{\eta}^T\boldsymbol{B}\boldsymbol{L}^{-1}\boldsymbol{v} \right\} dt = 0 \tag{56}$$

This is the Hamilton's principle expression from which we will derive our motion equations. Now, performing the variation on the variables $\boldsymbol{v}$, $\boldsymbol{\lambda}$, $\boldsymbol{\eta}$ and $\boldsymbol{q}$ successively, we get:

– variation of $\boldsymbol{v}$ yields

$$-\boldsymbol{M}\boldsymbol{v} + \boldsymbol{M}\boldsymbol{L}\dot{\boldsymbol{q}} - \boldsymbol{L}^{-T}\boldsymbol{B}^T\boldsymbol{\eta} = \boldsymbol{0} \tag{57}$$

– variation of the multipliers $\boldsymbol{\lambda}$ restores the constraints set (1)

– variation of the multipliers $\boldsymbol{\eta}$ gives

$$\boldsymbol{B}\boldsymbol{L}^{-1}\boldsymbol{v} = \boldsymbol{0} \tag{58}$$

– variation of the generalized displacements $\boldsymbol{q}$ yields

$$\int_{t_1}^{t_2} \left\{ -\frac{\partial \mathcal{V}}{\partial \boldsymbol{q}}\delta\boldsymbol{q} - \left(\frac{\partial \boldsymbol{\Phi}}{\partial \boldsymbol{q}}\right)^T \boldsymbol{\lambda} + \delta\dot{\boldsymbol{q}}(\boldsymbol{L}^T\boldsymbol{M}\boldsymbol{v}) + \delta\boldsymbol{q}\frac{\partial}{\partial \boldsymbol{q}}\left[(\boldsymbol{L}\dot{\boldsymbol{q}})^T\boldsymbol{M}\boldsymbol{v}\right] \right\} dt = 0 \tag{59}$$

from which the dynamic equilibrium equations will be extracted.

Integration by parts of Eq. (59) yields

$$L^T M \dot{v} + G(Mv)\dot{q} + \frac{\partial \mathcal{V}}{\partial q} + B^T \lambda = 0 \tag{60}$$

Then the equations of motion become a first order DAE system with q, v, λ and η as variables:

$$\begin{cases} L^T M \dot{v} + G\dot{q} + \dfrac{\partial \mathcal{V}}{\partial q} + B^T \lambda = 0 \\ -L^T M v + L^T M L \dot{q} - B^T \eta = 0 \\ \Phi = 0 \\ B L^{-1} v = 0 \end{cases} \tag{61}$$

This formulation provides now the automatic enforcement of the velocity-level constraint besides the position-level one, thus eliminates the problem of drift for these constraints.

5.3.1   Discretization of the equation of motion

The interpolated displacements and velocities have the same expressions as in the previous scheme:

$$\begin{aligned} q &= \frac{(q_j + q_{n+1})}{2} + \tau \frac{(q_{n+1} - \alpha q_j - (1-\alpha)q_n)}{2} & \dot{q} &= \frac{(q_{n+1} - q_j)}{h} \\ v &= \frac{(v_j + v_{n+1})}{2} + \tau \frac{(v_{n+1} - \alpha v_j - (1-\alpha)v_n)}{2} & \dot{v} &= \frac{(v_{n+1} - v_j)}{h} \end{aligned} \tag{62}$$

In the same way, internal and constraint forces are interpolated:

$$\begin{aligned} \frac{\partial \mathcal{V}}{\partial q} &= \left. \frac{\partial \mathcal{V}}{\partial q} \right|_g + \frac{\tau}{2} \left[\left. \frac{\partial \mathcal{V}}{\partial q} \right|_{n+1} - \alpha \left. \frac{\partial \mathcal{V}}{\partial q} \right|_j - (1-\alpha) \left. \frac{\partial \mathcal{V}}{\partial q} \right|_n \right] \\ B^T \lambda &= B_g^T \lambda_g + \frac{\tau}{2} \left(B_{n+1}^T \lambda_{n+1} - B_j^T \lambda_j \right) \\ B^T \eta &= B_g^T \eta_g + \frac{\tau}{2} \left(B_{n+1}^T \eta_{n+1} - B_j^T \eta_j \right) \end{aligned} \tag{63}$$

The Time Discontinuous Galerkin approximation of equations (61) writes

$$\int_{-1}^{1} \mathcal{W}_1(\tau) \left[\dot{q} - L^{-1} M^{-1} L^{-T} B^T \eta - L^{-1} v \right] d\tau +$$

$$\int_{-1}^{1} \mathcal{W}_2(\tau) \left[M\dot{v} + L^{-T} G\dot{q} + L^{-T} B^T \lambda + L^{-T} \frac{\partial \mathcal{V}}{\partial q} \right] d\tau +$$

$$\mathcal{W}_1(-1)(q_j - q_n) + \mathcal{W}_2(-1)[M(v_j - v_n) + L^{-T} G_h(q_j - q_n)] = 0 \tag{64}$$

where

$$\mathcal{W}_1(\tau) = A_1 + B_1\tau \qquad \mathcal{W}_2(\tau) = A_2 + B_2\tau \tag{65}$$

Integration of this expression leads to the discrete equations system formed by the equilibrium equations, the velocities/displacements relationships and the constraints at displacement-level and at velocity-level:

$$
\begin{cases}
\dfrac{1}{h}\boldsymbol{L}^T\boldsymbol{M}(\boldsymbol{v}_{n+1} - \boldsymbol{v}_n) + \dfrac{1}{h}\boldsymbol{G}_m(\boldsymbol{q}_{n+1} - \boldsymbol{q}_n) + \left.\dfrac{\partial\mathcal{V}}{\partial\boldsymbol{q}}\right|_g + (\boldsymbol{B}^T\boldsymbol{\lambda})_g = \boldsymbol{0} \\[3mm]
\dfrac{1}{h}\boldsymbol{L}^T\boldsymbol{M}(\boldsymbol{v}_j - \boldsymbol{v}_n) + \dfrac{1}{h}\boldsymbol{G}_h(\boldsymbol{q}_j - \boldsymbol{q}_n) - \\[3mm]
\qquad\qquad \dfrac{1}{3}\left[\left.\dfrac{\partial\mathcal{V}}{\partial\boldsymbol{q}}\right|_g - \left.\dfrac{\partial\mathcal{V}}{\partial\boldsymbol{q}}\right|_h\right] + \dfrac{1}{6}\alpha\left[\left.\dfrac{\partial\mathcal{V}}{\partial\boldsymbol{q}}\right|_j - \left.\dfrac{\partial\mathcal{V}}{\partial\boldsymbol{q}}\right|_n\right] - \dfrac{1}{3}(\boldsymbol{B}_g^T\boldsymbol{\lambda}_g - \boldsymbol{B}_h^T\boldsymbol{\lambda}_j) = \boldsymbol{0} \\[3mm]
\dfrac{1}{h}\boldsymbol{L}^T\boldsymbol{M}\boldsymbol{L}(\boldsymbol{q}_{n+1} - \boldsymbol{q}_n) - \boldsymbol{B}_g^T\boldsymbol{\eta}_g - \dfrac{\kappa}{2}\boldsymbol{L}^T\boldsymbol{M}\boldsymbol{v}_{n+1} + \boldsymbol{v}_j = \boldsymbol{0} \\[3mm]
\dfrac{1}{h}\boldsymbol{L}^T\boldsymbol{M}\boldsymbol{L}(\boldsymbol{q}_j - \boldsymbol{q}_n) + \dfrac{1}{6}(\boldsymbol{B}_{n+1}^T\boldsymbol{\eta}_{n+1} - \boldsymbol{B}_j^T\boldsymbol{\eta}_j) + \dfrac{\kappa}{6}\boldsymbol{L}^T\boldsymbol{M}(\boldsymbol{v}_{n+1} - \alpha\boldsymbol{v}_j - (1-\alpha)\boldsymbol{v}_n) = \boldsymbol{0} \\[3mm]
\boldsymbol{\Phi}_j(\boldsymbol{q}) = \boldsymbol{0} \\[2mm]
\boldsymbol{\Phi}_{n+1}(\boldsymbol{q}) = \boldsymbol{0} \\[2mm]
\boldsymbol{B}_j\boldsymbol{L}^{-1}\boldsymbol{v}_j = \boldsymbol{0} \\[2mm]
\boldsymbol{B}_{n+1}\boldsymbol{L}^{-1}\boldsymbol{v}_{n+1} = \boldsymbol{0}
\end{cases}
$$

$$\tag{66}$$

for $0 \leq \alpha \leq 1$.

We introduced an algorithmic parameter κ that will be adjusted to verify energy preservation in the case $\alpha = 0$, as it is shown in the next section. This parameter is $\kappa = 1 + O(\Delta t)$, that is

$$\lim_{\Delta t \to 0} \kappa = 1$$

for consistency. For $\alpha = 0$ we have a scheme that perfectly preserves the total energy of the system and for $\alpha = 1$ we reach the maximum energy dissipation.

5.3.2 Energy decay in the discrete scheme - computation of κ

Now we pre multiply (66-a) by $(\boldsymbol{q}_{n+1} - \boldsymbol{q}_n)^T$, (66-b) by $(\boldsymbol{q}_j - \boldsymbol{q}_n)^T$, (66-c) by $(\boldsymbol{v}_{n+1} - \boldsymbol{v}_n)^T\boldsymbol{L}^{-1}$ and (66-d) by $(\boldsymbol{v}_j - \boldsymbol{v}_n)^T\boldsymbol{L}^{-1}$. Combining linearly these four equations and after some algebra

we arrive at:

$$\frac{\kappa}{2}\left(\boldsymbol{v}_{n+1}^T\boldsymbol{M}\boldsymbol{v}_{n+1} - \boldsymbol{v}_n^T\boldsymbol{M}\boldsymbol{v}_n + \alpha\boldsymbol{v}_j^T\boldsymbol{M}\boldsymbol{v}_j - \alpha\boldsymbol{v}_j^T\boldsymbol{M}\boldsymbol{v}_n - \alpha\boldsymbol{v}_n^T\boldsymbol{M}\boldsymbol{v}_j + \alpha\boldsymbol{v}_n^T\boldsymbol{M}\boldsymbol{v}_n\right) +$$

$$(\boldsymbol{q}_{n+1}-\boldsymbol{q}_j)^T\left.\frac{\partial\mathcal{V}}{\partial\boldsymbol{q}}\right|_g + (\boldsymbol{q}_j-\boldsymbol{q}_n)^T\left.\frac{\partial\mathcal{V}}{\partial\boldsymbol{q}}\right|_h + (\boldsymbol{q}_j-\boldsymbol{q}_n)^T\frac{\alpha}{2}\left[\left.\frac{\partial\mathcal{V}}{\partial\boldsymbol{q}}\right|_j - \left.\frac{\partial\mathcal{V}}{\partial\boldsymbol{q}}\right|_n\right] + (\boldsymbol{q}_{n+1}-\boldsymbol{q}_j)^T\boldsymbol{B}_g^T\boldsymbol{\lambda}_g +$$

$$(\boldsymbol{q}_j - \boldsymbol{q}_n)^T\boldsymbol{B}_h^T\boldsymbol{\lambda}_j + \boldsymbol{\eta}_g^T\boldsymbol{B}_g\boldsymbol{L}^{-1}(\boldsymbol{v}_{n+1} - \boldsymbol{v}_n) - \frac{1}{2}(\boldsymbol{\eta}_{n+1}^T\boldsymbol{B}_{n+1} - \boldsymbol{\eta}_j^T\boldsymbol{B}_j)\boldsymbol{L}^{-1}(\boldsymbol{v}_j - \boldsymbol{v}_n) = 0 \quad (67)$$

The work done by the gyroscopic forces is null because of the skew-symmetry of $\boldsymbol{G}_m$ and $\boldsymbol{G}_h$, as it was said in the previous sections.

By identifying the different energy terms and grouping them together, we get:

$$\kappa\left[\mathcal{K}_{n+1} - \mathcal{K}_n + \frac{\alpha}{2}(\boldsymbol{v}_j - \boldsymbol{v}_n)^T\boldsymbol{M}(\boldsymbol{v}_j - \boldsymbol{v}_n)\right] +$$

$$\mathcal{V}_{n+1} - \mathcal{V}_n + (\boldsymbol{q}_j - \boldsymbol{q}_n)^T\frac{\alpha}{2}\left[\left.\frac{\partial\mathcal{V}}{\partial\boldsymbol{q}}\right|_j - \left.\frac{\partial\mathcal{V}}{\partial\boldsymbol{q}}\right|_n\right] +$$

$$\boldsymbol{\eta}_g^T\boldsymbol{B}_g\boldsymbol{L}^{-1}(\boldsymbol{v}_{n+1} - \boldsymbol{v}_n) - \frac{1}{2}(\boldsymbol{\eta}_{n+1}^T\boldsymbol{B}_{n+1} - \boldsymbol{\eta}_j^T\boldsymbol{B}_j)\boldsymbol{L}^{-1}(\boldsymbol{v}_j - \boldsymbol{v}_n) = \boldsymbol{0} \quad (68)$$

where we have used again the concept of *discrete directional derivative*, as we did in the previous sections, replacing the expressions $(\partial\mathcal{V}/\partial\boldsymbol{q})_g$ and $(\partial\mathcal{V}/\partial\boldsymbol{q})_h$ by the discrete counterparts in order to verify the expressions (35). Matrices $\boldsymbol{B}_g$ and $\boldsymbol{B}_h$ are approximated with $\boldsymbol{B}_g^*$ and $\boldsymbol{B}_h^*$ in order to satisfy (37).

Now we have that for $\alpha = 0$ the algorithmic total energy of the system must be perfectly preserved, that is:

$$\kappa(\mathcal{K}_{n+1} - \mathcal{K}_n) + (\mathcal{V}_{n+1} - \mathcal{V}_n) +$$

$$\frac{1}{2}\left[\boldsymbol{\eta}_j^T\boldsymbol{B}_j\boldsymbol{L}^{-1}(\boldsymbol{v}_{n+1} + \boldsymbol{v}_j - 2\boldsymbol{v}_n) + \boldsymbol{\eta}_{n+1}^T\boldsymbol{B}_{n+1}\boldsymbol{L}^{-1}(\boldsymbol{v}_{n+1} - \boldsymbol{v}_j)\right] = \boldsymbol{0} \quad (69)$$

Then we obtain a closed form to compute the κ coefficient:

$$\kappa = -\frac{(\mathcal{V}_{n+1} - \mathcal{V}_n) + \frac{1}{2}\left[\boldsymbol{\eta}_j^T\boldsymbol{B}_j\boldsymbol{L}^{-1}(\boldsymbol{v}_{n+1} + \boldsymbol{v}_j - 2\boldsymbol{v}_n) + \boldsymbol{\eta}_{n+1}^T\boldsymbol{B}_{n+1}\boldsymbol{L}^{-1}(\boldsymbol{v}_{n+1} - \boldsymbol{v}_j)\right]}{(\mathcal{K}_{n+1} - \mathcal{K}_n)} \quad (70)$$

If the total energy of the system is preserved, we have that $\Delta\mathcal{K} + \Delta\mathcal{V} = 0$ from where $\Delta\mathcal{K} = -\Delta\mathcal{V}$. Then κ writes:

$$\kappa = 1 - \frac{\boldsymbol{\eta}_j^T\boldsymbol{B}_j\boldsymbol{L}^{-1}(\boldsymbol{v}_{n+1} + \boldsymbol{v}_j - 2\boldsymbol{v}_n) + \boldsymbol{\eta}_{n+1}^T\boldsymbol{B}_{n+1}\boldsymbol{L}^{-1}(\boldsymbol{v}_{n+1} - \boldsymbol{v}_j)}{2(\mathcal{K}_{n+1} - \mathcal{K}_n)} \quad (71)$$

We see that κ is a measure of the work done by the constraint forces at the velocity level with respect to the kinetic energy jump.
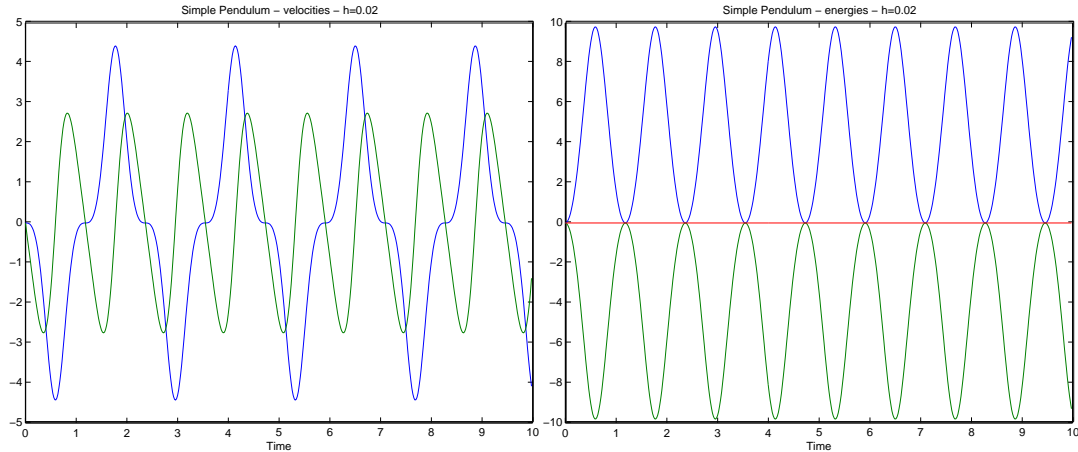
Figure 18: Simple pendulum: velocities and energies in cartesian coordinates for test case b (constrained model) and $\alpha = 0$

5.3.3   Numerical examples

Figure 18 shows that now this scheme works well in both cases: constrained and unconstrained. The locking problem has disappeared. In addition, the amount of energy dissipated increases monotonously with α for the constrained case and the values are now 1000 times lower than before, for the case of $\alpha = 1$. Figure 20 shows different plots of the evolution of the parameter κ, for $\alpha = 0$ and $\alpha = 1$, constrained case, and for a time step size $h = 0.02$.
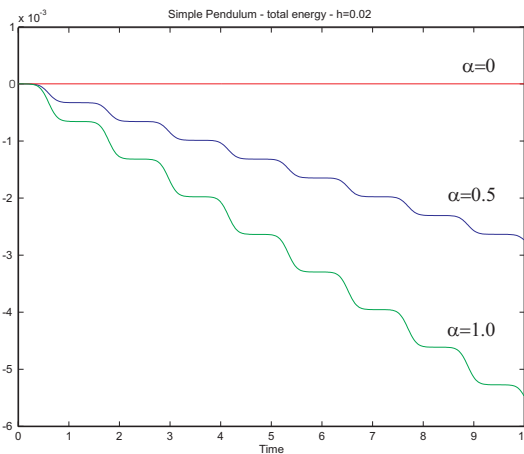

Figure 19: Simple pendulum: time evolution of total energy for different values of α for the constrained model (test case b)
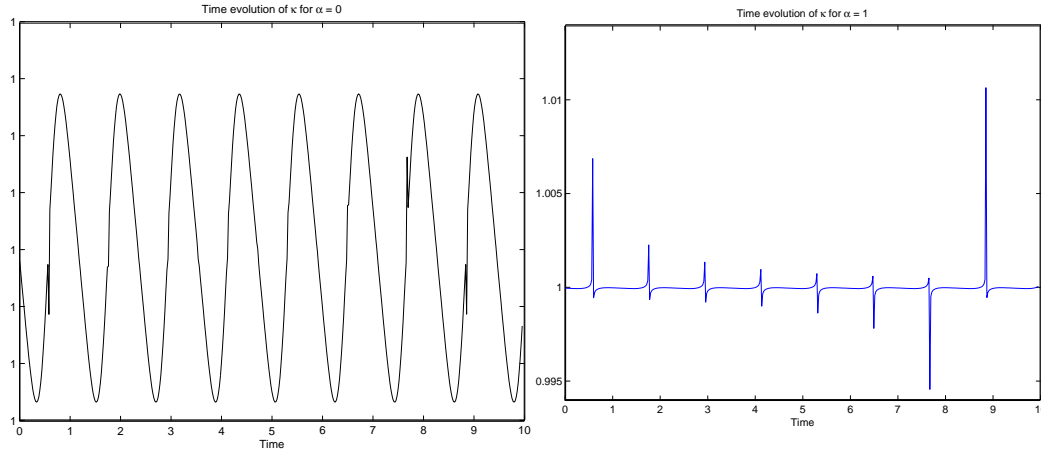
Figure 20: Simple pendulum: time evolution of κ coefficient for $\alpha = 0$ and $\alpha = 1$ for the test case b (constrained model)

5.3.4   Conclusions

A new algorithm for nonlinearly constrained DAEs that controls the amount of energy dissipation has been proposed where displacement constraints and their time derivatives have been imposed. Independent interpolation of displacements and velocities are used and constraints at velocity level are introduced to avoid the locking phenomenon. The proposed scheme uses the concept of discrete derivatives[6] to get energy conservation. The most common holonomic type of constraints are taken into consideration in the examples.

6   CONCLUSIONS

A variety of time integration schemes for constrained multibody dynamics were analyzed.

Discretization processes were developed for elastic and inertial forces in order to achieve the corresponding preservation or dissipation of the total mechanical energy of the system at the discrete solution level.

A discretization process was developed also for the constrained forces, in order to guarantee the exact satisfaction of nonlinear constraints and the vanishing of the work performed by the constraint forces.

It has been shown that in spite of Energy Preserving Scheme provides nonlinear unconditional stability for MBS, it lacks the high-frequency numerical dissipation required to tackle realistic engineering problems which many times can lead to the damage of the computation. The high frequency numerical dissipation is imperative for time integration in multibody systems, in order to assure the stability of the solution.

It has been shown that constraints and time derivatives of constraints should be both imposed when using independent interpolation of displacements and velocities to avoid locking.

REFERENCES

[1] A. Cardona. *An Integrated Approach to Mechanism Analysis*. PhD thesis, Faculté des Sciences Appliquées, Université of Liège, Belgique, (1989).

[2] J. Chung and G. M. Hulbert. A time integration algorithm for structural dynamics with improved numerical dissipation: the generalized α method. *Journal of Applied Mechanics*, **60**, 371–375 (1993).

[3] C. Johnson. *Numerical Solution of Partial Differential Equations by the Finite Element Method*. Cambridge University Press, Cambridge, (1994).

[4] E. Lens, A. Cardona, and M. Géradin. Energy preserving time integration for constrained multibody systems. *Multibody System Dynamics*, **11**, 41–61 (2004).

[5] M. Géradin and A. Cardona. *Flexible Multibody Dynamics: a Finite Element Approach*. John Wiley & Sons Ltd, (2000).

[6] O. Gonzalez. Mechanical systems subject to holonomic constraints: differential-algebraic formulations and conservative integration. *Physica D*, **132**, 165–174 (1999).

[7] C. W. Gear, B. Leimkuhler, and G. K. Gupta. Automatic integration of euler-lagrange equations with constraints. *Journal of Computational and Applied Mathematics*, **12-13**, 77–90 (1985).